The Role of Schlemm's Canal in Aqueous Outflow from the Human Eye

M. C. Johnson and R. D. Kamm

A mathematical model of Schlemm's canal is developed to simulate collapse of the canal and its effect on resistance to flow through the aqueous outflow network. Schlemm's canal is modeled as a porous, compliant channel that is held open by the trabecular meshwork. The trabecular meshwork is modeled as a series of linear springs that allow the inner wall of Schlemm's canal to deform in proportion to the local pressure drop across it. Based on comparisons between the model and results in the literature, the following tentative conclusions are reached: (1) Most of the resistance in the aqueous outflow network occurs in the inner wall of Schlemm's canal. (2) Glaucoma is not caused by a weakening of the trabecular meshwork and a resultant collapse of Schlemm's canal alone. Instead, glaucoma probably results from an increased flow resistance of the inner wall of the canal. Invest Ophthalmol Vis Sci 24:320–325, 1983

Aqueous humor flows through the outflow network at an extremely low flow rate (2.0 μl/min), yet this flow produces a surprisingly large pressure drop over a short flow distance (less than 1 mm). The pressure drop is around 6 mmHg in normal eyes and can be as much as 40 mmHg in glaucomatous eyes. In order to achieve a better understanding of the outflow network, changes in which can lead to ocular hypertension and glaucoma, we studied the role of Schlemm's canal in producing a pressure drop in the normal eye.

Many studies have sought to determine the principal site of flow resistance in the aqueous outflow network. Toward this end, numerous perfusion studies have been conducted, the results of which indicate that the relationship between pressure and flow is nearly linear with flow resistance increasing slowly with pressure.[1]

A number of sites have been identified as possible sources of resistance: (1) corneoscleral meshwork, (2) juxtacanalicular meshwork, (3) endothelial lining of the inner wall of Schlemm's canal, (4) Schlemm's canal, and (5) collector channels and aqueous veins.

Two considerations preclude the *corneoscleral meshwork* from being the principal site of flow resistance: (1) the size of the openings in the corneoscleral meshwork is too large to cause an appreciable resistance,[2] and (2) Johnstone and Grant[3] showed that as IOP increases, the spaces in the trabecular meshwork expand. As the spaces open, the hydrodynamic resistance would decrease. Thus, if the corneoscleral meshwork were the principal site of flow resistance, one would expect the resistance to decrease rather than increase with an increase in IOP.

The *aqueous veins* are much too large to cause any appreciable resistance. Stresses in the sclera due to IOP could conceivably cause collapse of the aqueous veins (and thus generate significant flow resistance), but a recent study indicates that this does not occur until IOP is substantially elevated.[4]

The *juxtacanalicular meshwork and the endothelial lining of the inner wall of Schlemm's canal* are jointly considered as *the inner wall of Schlemm's canal* for this study. We have grouped these two regions together, in part, because there seems to be no general consensus concerning the mechanism of aqueous humor transport through them, and in part because our primary intent is to examine the effect of Schlemm's canal collapse by itself. It appears likely that the principal site of flow resistance is the *inner wall of Schlemm's canal*, or *Schlemm's canal*, or both. In this study, therefore, we develop a theoretical model that includes the flow resistance of both, and accounts only for the variations in flow resistance associated with collapse of the canal.

A Model of Schlemm's Canal as a Porous, Compliant Channel

Theoretical Model

Moses[5] modeled Schlemm's canal as a porous, rigid channel. From the predictions of his model, he con-

From the Department of Mechanical Engineering, Massachusetts Institute of Technology, Cambridge, Massachusetts.

Supported by a grant from the National Eye Institute (Grant #1 R01 Ey 03141-01).

Presented in part at the annual meeting of the Association for Research in Vision and Ophthalmology, Sarasota, Florida, 1981.

Submitted for publication November 23, 1981.

Reprint requests: Prof. Roger Kamm, Room 3-258, Massachusetts Institute of Technology, 77 Massachusetts Avenue, Cambridge, MA 02139.

0146-0404/83/0300/320/$1.10 © Association for Research in Vision and Ophthalmology

cluded that Schlemm's canal contributes little to the total flow resistance until it is greatly collapsed. However, his model did not allow canal dimensions to change with IOP, and thus could neither determine the state of collapse of the canal, nor demonstrate the change in outflow resistance associated with this collapse as IOP is elevated.

In our flow model, depicted in Figure 1, aqueous humor flows from the trabecular meshwork (TM) through the inner wall, into Schlemm's canal, along the canal in the circumferential direction, and exits through one of 30 equally spaced collector channels (only the portion of the canal between two collector channels is shown in Figure 1). The trabecular meshwork is represented by a series of linear springs that allow the inner wall to deform in proportion to the local pressure drop across it; the inner wall is flexible and is supported by the meshwork attachment while the outer wall is assumed rigid.

The fluid pressure is assumed constant (and equal to IOP) until the aqueous humor passes through the inner wall, which is assumed to have a constant conductance per unit length ($1/R_w$) along the canal. The incremental flow entering the canal at any location is determined by the pressure drop across the inner wall at that point and by the flow resistance of the inner wall:

$$dQ(x)/dx = [IOP - P(x)]/R_w. \quad (1)$$

The distance along the canal (x) is measured from the midpoint between two adjacent collector channels. P(x) and Q(x) represent, respectively, the pressure and flow rate at location x in the canal.

Assuming that the height* of the canal (h(x)) varies slowly with position and is typically much smaller than the canal width (the meridional diameter of Schlemm's canal), the flow can be modeled as quasi-rectilinear flow between two nearly parallel sheets (the inner and outer wall). Furthermore, recognizing that the Reynolds number of the flow is much less than one and hence the flow is inertia-free, the following relationship can be obtained from a force balance[6]:

$$dP(x)/dx = 12\mu Q(x)/wh^3(x). \quad (2)$$

Here w is the width of Schlemm's canal and μ is the viscosity of aqueous humor.

As suggested by Figure 1, the inner wall is held away from the outer wall by a network of linear springs that allow the inner wall to deform in proportion to the local pressure drop across it. The displacement of these springs is described as follows:

$$[h(x) - h_0]/h_0 = [P(x) - IOP]/E \quad (3)$$

where E is the elastic modulus (or stiffness) of the springs and h_0 is the undeformed height of the canal (the height when IOP equals collector channel pressure).

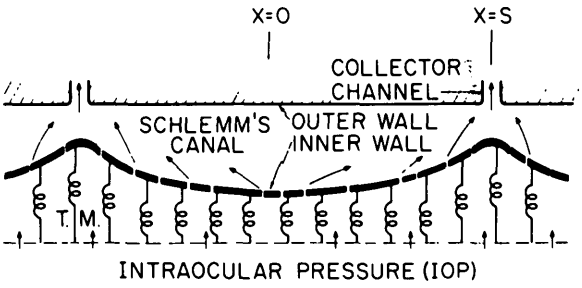

Fig. 1. Model of Schlemm's canal as a porous, compliant channel. The height of the channel has been exaggerated.

Two boundary conditions are applied (Fig. 1): (a) by symmetry, there is no circumferential flow in Schlemm's canal at the point halfway between collector channels (x = 0). (b) The pressure at x = s (the collector channel pressure—P_{cc}) is specified.

$$\text{(a) } Q(0) = 0$$

$$\text{(b) } P(s) = P_{cc}$$

It is convenient here to introduce several nondimensional variables. They serve to simplify the form of the final equation.

$x' \equiv x/s$: the nondimensional distance along the canal.

$H(x') \equiv h(x)/h_0 = 1 - [IOP - P(x)/E$: the nondimensional canal height. It varies between zero (totally collapsed) and one (the undeformed state).

$\mathcal{P} \equiv (IOP - P_{cc})/E$: the nondimensional pressure drop of the system. $1 - \mathcal{P}$ is the nondimensional height at the collector channel.

$\beta^2 = \dfrac{12\mu s/wh_0^3}{R_w/s}$: the ratio between the resistance in the undeformed canal and the resistance of the inner wall.

Introducing these nondimensional variables and combining Equations (1)–(3) yields a single governing differential equation:

$$\beta^2[H(x') - 1] = H^3(x')\, d^2H(x')/dx'^2 + 3H^2(x')[dH(x')/dx']^2 \quad (4)$$

and boundary conditions:

$$dH(0)/dx' = 0 \quad (4a)$$

$$H(1) = 1 - \mathcal{P}. \quad (4b)$$

* Moses[5] uses "width" to denote the distance between the inner wall and the outer wall of the canal. We here use "height" to denote this distance.

Table 1. Typical values of the parameters of the human aqueous outflow network

Parameter	*Description*	*Typical value*	*Reference*
Q_{TOTAL}	Flow through the conventional outflow pathway	2.4 μl/min	Moses[5]
IOP	Intraocular pressure	15 mmHg	
P_{cc}	Collector channel pressure (assumed equal to episcleral venous pressure)	9 mmHg	
ΔP	Pressure drop (IOP-P_{cc})	6 mmHg	
n	Number of collector channels	30	Moses[5]
Q	Flow through each side of the collector channel (2Q enters each collector channel)	0.04 μl/min	
μ	Viscosity of aqueous humor @ 37 C	$7.5 \times 10^{-4} \frac{kg}{m\ sec}$	Moses[5]
2s	Length of canal between two collector channels	1200 μm	
w	Width of the canal	300 μm	Moses[5]
h_0	Undeformed height of the canal	25 μm	Johnstone & Grant[3]
R_w/s	Inner wall resistance on one side of a collector channel (~ ΔP/Q)	$150 \frac{mmHg}{\mu l/min}$	See text
E	Modulus of the trabecular meshwork	20 mmHg	Johnstone & Grant[3]
β^2	The ratio between the resistance to flow in Schlemm's canal in the undeformed state, and the resistance to flow through the inner wall of Schlemm's canal	9×10^{-4}	
$\mathcal{P}$	$\frac{\text{Pressure drop}}{\text{Modulus of TM}}$	0.3	

Note that two parameters, β and $\mathcal{P}$, completely determine the character of H(x'). Using numerical methods,[7] we have determined the solutions to this equation for $0.01 < \beta < 0.5$ and $0 < \mathcal{P} < 1$.

Results

Typical values of the various parameters are shown in Table 1. R_w/s is estimated by assuming all the flow resistance at normal IOP is due to inner wall resistance; thus, as shown in the table: $R_w/s \sim \Delta P/Q$. E and h_0 are estimated using micrographs of the outflow network obtained at different IOPs.[3]

Each of the graphs in this paper has a double set of axes: the inner axis will show the nondimensional coordinates, while the outer axis will show dimensional coordinates that are found using the typical values of the parameters shown in Table 1.

Figure 2 shows the height of the canal as a function of distance along the canal for several different values of pressure drop. Note that at normal IOP ($\mathcal{P} = 0.3$), the canal is nearly wide open. As IOP is increased, the canal collapses with the greatest collapse occurring adjacent to the collector channel. Once the canal walls come into contact, the solution can be carried no further due to the restriction imposed by equation (2) that h(x) be greater than zero.

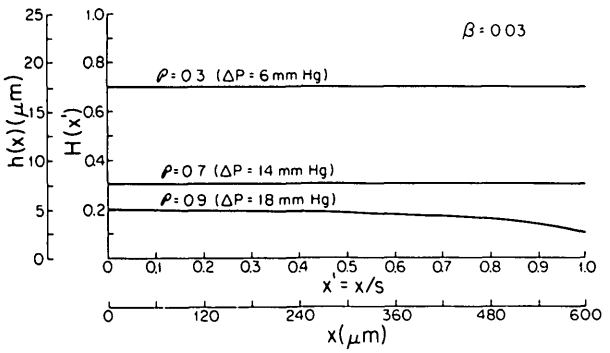

Fig. 2. Degree of collapse as a function of distance along the channel.

Figure 3 shows the flow rate entering a collector channel as a function of pressure drop for various values of β. $\bar{Q}$ is the nondimensional flow rate ($\bar{Q} \equiv \mu Q(s)s/wh_0^3 E$); Q_{TOTAL}, shown on the outer axis, is the total dimensional flow entering all 30 collector channels. The curves indicate that at low IOP the resistance to flow is *constant*, but as IOP is increased, canal collapse becomes significant and flow resistance increases. It is because β is small that the outflow resistance changes only slightly with IOP; most of the resistance is in the inner wall and, by assumption, is constant; the resistance within the canal changes dramatically as the canal collapses, but it is only a small part of the total resistance until the canal is almost completely collapsed.

Complete Collapse of the Canal Prevented by Septae

Theoretical Model

The model introduced in the previous section has a problem when $\mathcal{P} = 1$: this corresponds to total collapse of the canal at the collector channel and generates an infinite flow resistance per unit length. However, this is unlikely to occur due to the presence of septae (or endothelial tubules) in Schlemm's canal as have been observed by many investigators.[8,9] The septae are concentrated near collector channels where our model predicts collapse would first occur and where they would therefore be of greatest value. John-

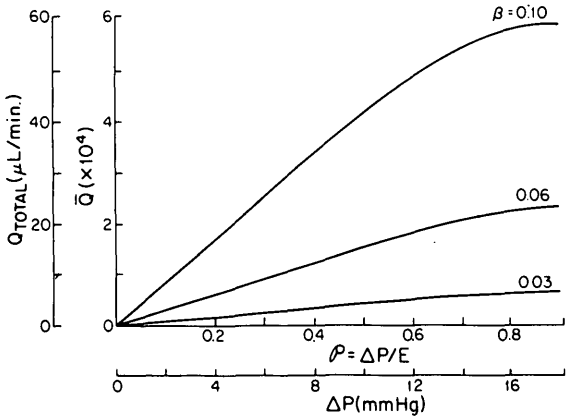

Fig. 3. Flow rate vs pressure drop for the porous, compliant channel.†

stone (personal communication) has estimated that there are 2000 endothelial tubules in the eye. Other factors may also prevent complete collapse of the canal such as the existence or persistence of a pocket at the posterior portion of the canal near the scleral spur. In this paper we consider only the effects of septae in preventing complete collapse. We expect qualitatively similar results to those described in this section if complete collapse is prevented by other factors.

In this section, we model the septae as supporting members that inhibit Schlemm's canal from further collapse when the canal has sufficiently collapsed for the supporting members to become effective (hereafter the effective height of the supporting members is referred to as the support height). The support height would probably be approximately equal to the the septae diameter. For the purpose of this analysis, the supporting members are assumed to be distributed uniformly along the canal.

Unlike the situation described in the previous section for which one dimensionless solution described the entire range of pressure, the addition of septae gives rise to three separate flow regimes (Fig. 4):

Regime I ($\mathcal{P} < \mathcal{P}_c$): The canal height is everywhere greater than the support height, and thus the canal behaves as the porous, compliant channel described in the previous section.

Regime II ($\mathcal{P}_c < \mathcal{P} < \mathcal{P}_R$): Within this range of $\mathcal{P}$ the canal can be divided into two regions (Fig. 5): one, extending from $x' = 0$ to $x' = x_c$ where the canal has a height greater than the support height and behaves as the porous, compliant channel of the previous section; and the other extending from $x' = x_c$ to $x' = 1$ where the canal is collapsed to the support height and behaves as a porous, rigid channel. The

† The flow rates considered are extended well beyond the physiologic range but are necessary to clearly illustrate the nature of flow resistance at high degrees of canal collapse.

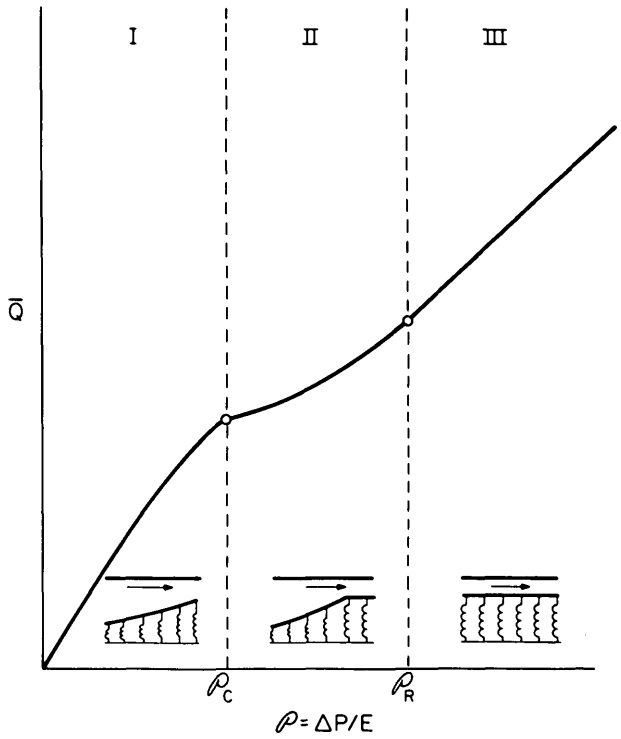

Fig. 4. Schematic of typical pressure-flow curve for the rigid septae model. Sketches show channel geometry for each of the three regimes.

flow solution in these two regions can be linked to solve for the overall pressure-flow relationship in Regime II.[7]

Regime III ($\mathcal{P} > \mathcal{P}_R$): The canal height is everywhere collapsed to the support height, and therefore constrained from further collapse. The results in this regime are similar to those obtained in the rigid channel model of Moses.[5] The only difference between the two models lies in the assumed cross-sectional shape of the canal that has only a small influence on the results.

Results

$\mathcal{P}_c$, the dimensionless pressure at which the septae first become important, is determined by the support height. $\mathcal{P}_c = (h_0 - h_s)/h_0$ where h_s is the support

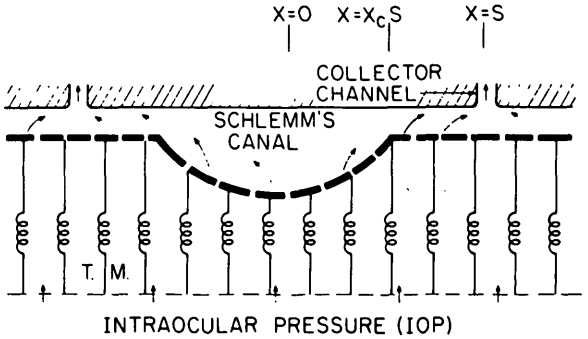

Fig. 5. Model of Schlemm's canal as a porous, compliant channel with complete collapse prevented by septae.

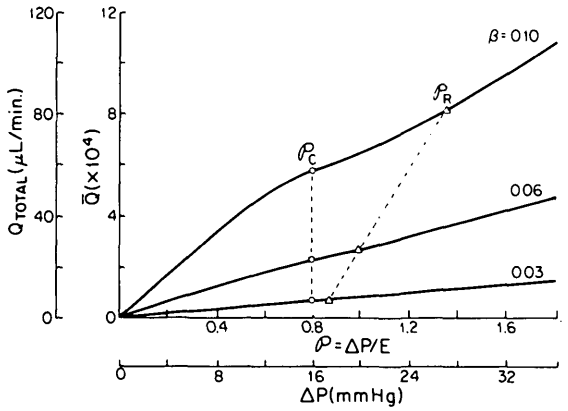

Fig. 6. Flow rate vs. pressure drop for the rigid septae model.†

height. If we choose the support height to be slightly less than the diameter of typical septae or about 5 μm, then the value of $\mathcal{P}_c$ would be 0.8. Figure 6 shows the pressure-flow curves for $\mathcal{P}_c = 0.8$. The outflow resistance is nearly constant until the canal is significantly collapsed whereupon further increases in IOP cause the resistance to increase, until the canal is everywhere collapsed to the support height. Above this pressure ($\mathcal{P}_R$) the canal is rigid and the resistance remains constant.

Glaucoma may result from an increase in the resistance of the inner wall thereby increasing total outflow resistance. This effect can be seen in Figure 7 as β is reduced from 0.03 to 0.015, which is equivalent to a fourfold increase in the inner wall resistance. Point A represents the preglaucomatous eye with a pressure drop of 6 mmHg; Point B represents the glaucomatous eye at the same flow rate but a pressure drop of 24.5 mmHg. If we assume an episcleral venous pressure of 9 mmHg, this would indicate a rise in IOP from 15 mmHg to 33.5 mmHg caused by the change in outflow resistance.

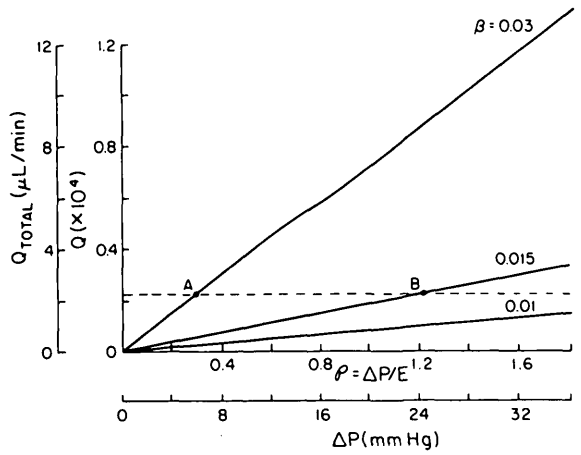

Fig. 7. Flow rate vs. pressure drop using typical values of a normal eye (**A**) and a glaucomatous eye (**B**).

Compliant Septae

The septae preventing complete collapse of Schlemm's canal are modeled above as completely rigid in that they prevent the canal from collapsing beyond the support height. Furthermore, it has been assumed that the inner wall does not collapse beyond the effective height of the septae even in between adjacent septae. We can simulate a somewhat more realistic situation by allowing the septae to be compliant such that the effective channel height can fall below the support height. We do this by making the linear springs of Figure 5 stiffer when the canal collapses past the support height. Three cases are shown in Figure 8: (1) the rigid septae model ($E_s = \infty$), (2) the modulus of the septae eight times as stiff as that of the trabecular meshwork ($E_s = 8E_{TM}$), and (3) four times as stiff ($E_s = 4E_{TM}$). Little difference is seen between the models until IOP is elevated substantially.

Discussion

Most experimental investigations have indicated that the outflow resistance increases as IOP is increased; however, the change in resistance is not dramatic (on average a resistance of 2.51 mmHg·min/μL at 10 mmHg increasing to 3.55 mmHg·min/μL at 50 mmHg[10]). In our model, we have assumed that the resistance has two components: the resistance to flow through the canal and the resistance to flow through the inner wall—the ratio of these two resistances is β^2.

The predictions of the model agree with the experimental observation of a nearly constant resistance if we select a value of β^2 much less than one (Fig. 3). We can restate this result as follows. If Schlemm's canal contributed significantly to the total outflow resistance, then changes in its dimensions—caused by changes in IOP—would lead to large changes in resistance. Since only small changes in resistance occur as IOP changes, Schlemm's canal resistance must be a small part of the total resistance. Therefore, we conclude that *most of the resistance in the aqueous outflow network occurs in the inner wall of Schlemm's canal.*

The nonlinearities in the pressure-flow curve predicted by our model are due to collapse of Schlemm's canal; however, it is possible that β is even smaller than we have assumed (perhaps less than 0.01) and that the nonlinearities observed are due to variations in the inner wall resistance, R_w. It would be possible to distinguish between these two possibilities if very precise pressure-flow data were available either from enucleated or living eyes. If canal collapse produced the observed change in resistance, then the experimental results would resemble the curves of Figure

3. If, on the other hand, changes in the inner wall led to the observed increase in outflow resistance, the changes would likely be more gradual and would begin as soon as the inner wall begins to deflect; that is, at very low values of IOP.

Our first model allowed for complete collapse of Schlemm's canal at high IOP. However, this would generate extremely high flow resistance that is not found experimentally. We modified our model to account for septae that prevent complete collapse of the canal. This modified model predicts a nearly constant resistance until the canal is significantly collapsed. Further increases in IOP collapse the canal to the height allowed by the compressed septae causing the resistance to rise. As IOP is increased further the canal collapses to its limit whereupon it becomes rigid and the resistance is again constant (see Figs. 4, and 6). Support for this model can be found in a study by Levene and Hyman.[11] They found resistance to increase as IOP increases; however, they found that resistance reached a maximum and remained nearly constant as IOP was further increased.

We also allowed the effective channel height to decrease below the effective septae height to simulate further compression of the septae or inner wall collapse in between adjacent septae. In view of the results of the Levene and Hyman study, the septae can be regarded as being fairly rigid once they are compressed or buckled.

One limitation of the model that should be mentioned is the assumption that the various parameters such as E, h_0, and β are the same for all 30 collector channels. Actually, statistical variations in the parameters will occur around the circumference of the eye. This will not qualitatively change the features of the model but will smooth the transition between Regimes I, II, and III shown in Figure 4.

A rise in IOP or a weakening of the trabecular meshwork would cause a distension of the trabecular meshwork and a collapse of Schlemm's canal. The septae prevent complete collapse, which would generate a very high outflow resistance. Johnstone and Grant[3] showed that the trabecular meshwork is completely expanded, and Schlemm's canal is completely collapsed (with septae providing occasional openings) at 50 mmHg. Yet the outflow resistance at 50 mmHg, measured by several investigators,[10,12] is not high enough to cause glaucoma. We conclude that *glaucoma is not caused by a weakening of the trabecular meshwork and a resultant collapse of Schlemm's canal alone.*

Two possible explanations are proposed: although weakening of the trabecular meshwork alone would not cause glaucoma, a concurrent weakening of the septae, which normally prevent collapse of the canal, could. However, a seemingly more likely possibility is that glaucoma is caused by an increase of inner wall resistance.

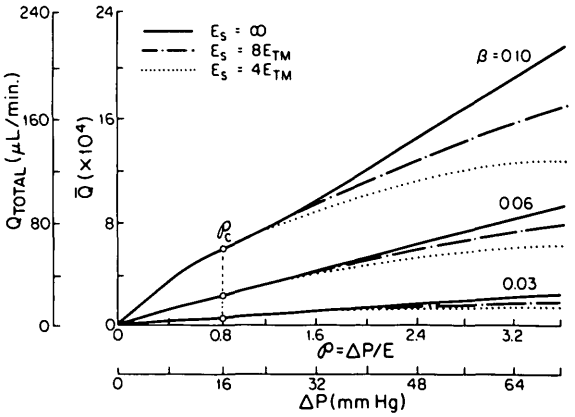

Fig. 8. Flow rate vs. pressure drop for the compliant septae model.†

Key words: Schlemm's canal, aqueous outflow, intraocular pressure, canal of Schlemm collapse, facility of outflow, cause of glaucoma, inner wall of Schlemm's canal

References

1. Moses RA: The effect of intraocular pressure on resistance to outflow. Surv Ophthalmol 22:88, 1977.
2. McEwen WK: Application of Poiseuille's law to aqueous outflow. Arch Ophthalmol 60:290, 1958.
3. Johnstone MA and Grant WM: Pressure-dependent changes in structures of the aqueous outflow system of human and monkey eyes. Am J Ophthalmol 75:365, 1973.
4. Battaglioli JL: The role of vessel collapse on the flow of aqueous humor. Masters Thesis, Department of Mechanical Engineering, MIT, June 1981.
5. Moses RA: Circumferential flow in Schlemm's canal. Am J Ophthalmol 88:585, 1979.
6. Schlichting H: Boundary Layer Theory. New York, McGraw-Hill, 1968, p. 77.
7. Johnson MC: The role of Schlemm's canal in aqueous outflow from the human eye. Masters Thesis, Department of Mechanical Engineering, MIT, June 1981.
8. Johnstone MA: Pressure-dependent changes in configuration of the endothelial tubules of Schlemm's canal. Am J Ophthalmol 78:630, 1974.
9. Hoffman F and Dumitrescu L. Schlemm's canal under the scanning electron microscope. Ophthalmic Res 2:37, 1971.
10. Brubaker RF: The effect of intraocular pressure on conventional outflow resistance in the enucleated human eye. Invest Ophthalmol 14:286, 1975.
11. Levene R and Hyman B: The effect of intraocular pressure on the facility of outflow. Exp Eye Res 8:116, 1969.
12. Hashimoto JM and Epstein DL: Influence of intraocular pressure on aqueous outflow facility in enucleated eyes of different mammals. Invest Ophthalmol Vis Sci 19:1483, 1980.